

A Histological Study of Enamel Developmental Defects in a Chacma Baboon (*Papio ursinus*) Incisor

Jamal K. Salaymeh^{1*}, Jimmy Erkens¹, Esme Beamish², W. Scott McGraw¹, Debbie Guatelli-Steinberg¹, Kate McGrath^{1,3,4}

¹ Department of Anthropology, The Ohio State University

² Institute for Communities and Wildlife in Africa (iCWild), University of Cape Town

³ Department of Anthropology, SUNY Oneonta

⁴ Center for the Advanced Study of Human Paleobiology, Department of Anthropology, The George Washington University

Keywords: dental histology, linear enamel hypoplasia, accentuated lines

ABSTRACT Physiological stress disrupts normal tooth growth creating grooves on the enamel surface (i.e., linear enamel hypoplasia or LEH). Hypoplastic defects often, but not always, co-occur with internal accentuated lines (AL). Monkeys reportedly exhibit fewer enamel defects than hominoids as their presumably faster-growing teeth produce shallower LEH defects that are harder to macroscopically identify. In this case study of a chacma baboon (*Papio ursinus*) incisor, we assessed whether AL are matched by LEH defects; how enamel extension rates (EER) and striae angles relate to the surface distribution of LEH defects; and whether striae angles are acute and EERs fast compared to hominoid anterior teeth. Normal wear to this specimen resulted in enamel loss (first two deciles) and surface abrasion, mainly near the cusp. We found a higher occurrence of AL (N = 48) compared to LEH defects (N = 10), which co-occurred in all instances of LEH. The spatial distribution of AL is more consistent, ranging from 3-10/decile, while LEH defects occur mainly in the midcrown and cervical regions. This incisor exhibits faster EERs (mean = 23.6 $\mu\text{m}/\text{day}$) and acuter striae angles (11-16°) compared to hominoids, likely creating shallower LEH defects and contributing to the discrepancy between AL and LEH defects.

Some chacma baboons inhabiting South Africa's Cape Peninsula live in close proximity to human dwellings and tourist attractions (Hoffman and O'Riain, 2011). Human-modified environments have been shown to offer baboons the opportunity to find high-calorie foods in the form of crops or food waste, which is linked to more rest time and improved body condition (Strum, 2010). Each square kilometer of human-modified habitat on the Cape Peninsula can support almost five times the baboon population compared to a square kilometer of natural habitat (Hoffman and O'Riain, 2012). However, human-modified environments can expose baboons to more frequent, and often-aggressive, interactions with humans (Kansky and Gaynor, 2000) (Figure 1). Baboons that persistently exhibit behavior that threatens the safety and welfare of residents in the Cape Peninsula may be euthanized (Beamish and O'Riain, 2014), sometimes

leading to the extirpation of entire baboon troops (Skead, 1980).

Both physiological and behavioral responses to stress have been observed in chacma baboons residing in Table Mountain National Park; adult baboons that spend more time in anthropogenic habitats have higher levels of glucocorticoid hormones, exhibit more aggressive behavior, and spend less time socializing (Chowdhury et al., 2020). Physiological stress during early development, such as bodily trauma, febrile illness, or malnutrition, is associated with disruptions in the normal enamel

*Correspondence to:
Jamal K. Salaymeh
The Ohio State University
Email: salaymeh.1@osu.edu



Figure 1. Left: female chacma baboon attempting to access food in a locked waste disposal bin (courtesy of Larissa Swedell). Right: male showing teeth in an act of intimidation (courtesy of Human Wildlife Solutions).

secretion activity (amelogenesis) of ameloblasts (Goodman and Rose, 1990; Guatelli-Steinberg et al., 2012; Hillson and Bond, 1997; Nanci, 2018). The present study focuses on two types of disruptions in enamel secretion: linear enamel hypoplasia and accentuated lines.

Linear enamel hypoplasia (LEH) manifests as horizontal grooves or lines that appears on the enamel surface (Goodman and Rose, 1990; Guatelli-Steinberg et al., 2012) (Figure 2). LEH defects often, but not always, co-occur with accentuated lines (AL) visible in the enamel cross-section (Condon and Rose, 1992; Witzel et al., 2008). The co-occurrence of the two defect types is expected, as it is thought that LEH and AL are external and internal manifestations of the same disruption in normal tooth growth (Goodman and Rose, 1990). However, a three threshold model for interpreting disturbances in enamel secretion at the cellular level has been set forth (Kierdorf et al., 2000; Kierdorf et al., 2004; Witzel et al., 2006; Witzel et al., 2008) and proposes an explanation for the variable co-occurrence of the two defect types: when the lowest threshold is surpassed, the minor disruption in growth can result in an LEH defect without the formation of a co-occurring accentuated line. They

also considered the timing of the disruption, arguing that accentuated lines are formed when all the involved ameloblasts are impaired, while LEH defects manifest when ameloblasts are disrupted during the late stage of secretion.

Accentuated lines manifest in enamel cross-sections as dark, pronounced lines that either fall between, or are coincident with, normal striae of Retzius (Guatelli-Steinberg, 2016). The latter structures form due to regular alterations in mineralization, mineral composition, or changes in the prism or crystalline structure of the enamel (Risnes, 1990), and represent a regular enamel growth rhythm, ranging from 2 to 12 days in primates (Dumont, 1995; Mahoney et al., 2017; McGrath et al., 2019).

It has been suggested that monkeys are less likely to exhibit LEH defects than great apes as the angles that their striae of Retzius make with the enamel surface are acute, leading to defects that are shallow and difficult to detect (Guatelli-Steinberg et al., 2012; McGrath et al., 2019). The acute striae angles in monkey teeth may represent fast rates of enamel extension, or the rate at which ameloblasts differentiate along the enamel-dentine junction (Shellis, 1998). Previous analyses in great

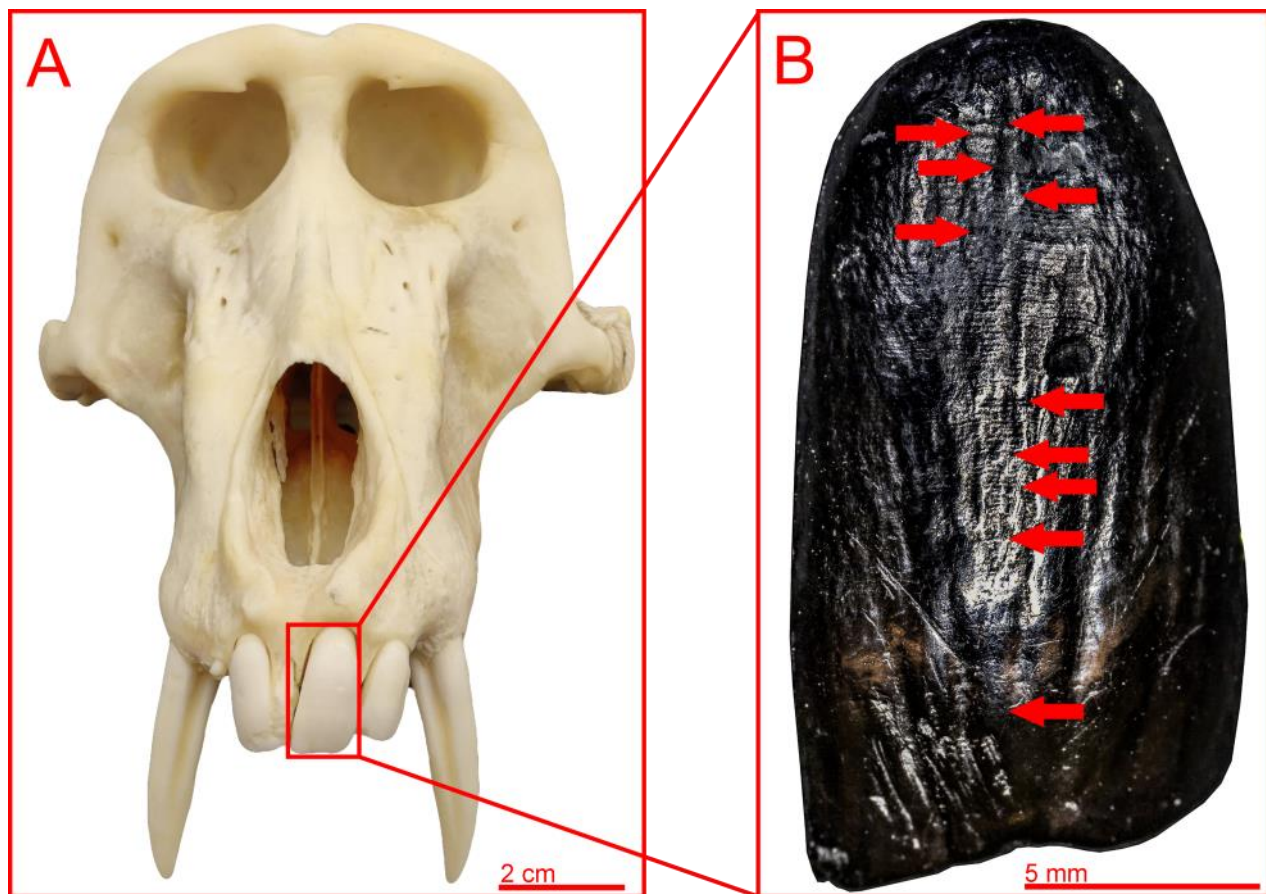


Figure 2. A: Cranium of male chacma baboon B4-03 with the sectioned incisor (ULI1) highlighted. B: Macro photograph of the incisor epoxy replica; red arrows mark the approximate locations of LEH defects (N = 10). Nine LEH defects were classified as minor; one defect (fifth LEH defect from the top of the image) was classified as moderate.

apes have documented strong relationships between faster enamel extension rates, acute striae angles just below the outer enamel surface (OES), and shallow LEH defects (McGrath et al., 2019). Enamel extension rates and associated striae angles change as enamel formation proceeds from cusp to cervix (Guatelli-Steinberg et al., 2012; McGrath et al., 2019; Shellis, 1998). Both human and nonhuman primate anterior teeth exhibit the highest enamel extension rates in the cuspal part of the crown, with reductions by the midcrown region. In humans, extension rates continue to decrease from the midcrown to the cervix. In nonhuman ape canines, extension rates remain constant, or in some cases, and particularly in males, increase toward the cervix (McGrath et al., 2019), with an associated decrease in the number of identified LEH defects in the last deciles (Guatelli-Steinberg et al., 2012). Less is known about the details of how enamel extension rates and striae angles change along the crowns of incisors, and currently no LEH defect depths exist for any monkey species. However, it

might be expected that monkeys with their faster life histories and relatively smaller body sizes should exhibit even faster enamel extension rates and acuter striae angles compared to hominoids.

Intrinsic growth variation influences LEH defect expression among species, sexes, and tooth types, while extrinsic variables like dental wear and abrasion add additional complications when interpreting imperfectly preserved teeth. Primate enamel is generally subject to considerable abrasion pressure that is attributed to the composition of their diet (Lucas et al., 2008) and the nature of their masticatory and extra-masticatory (e.g., using anterior teeth to grasp non-food items) tooth use behaviors (Molnar, 2011; Stojanowski et al., 2016). Incisor enamel is more susceptible to polishing and chipping compared to other tooth types (Stojanowski et al., 2016). This abrasion pattern is observed due to the anterior position of incisors in the skull, which provides the animal greater control when manipulating or processing dietary and non-dietary items using teeth (Stojanowski et al., 2016; Ungar, 1994).

This abrasion is exacerbated by the fact that many food items in baboon diets (especially hypogeous foods) are often contaminated with soil, sand, or other particulate matter, accelerating the wear rate of teeth by introducing exogenous grit to the oral cavity (Daegling and Grine, 1999; Galbany et al., 2014). Since normal tooth wear occurs mostly near the cusp, cuspal LEH defects may erode off the surface and become imperceptible, making them more challenging to identify compared to cervical LEH defects.

In the present study, a male chacma baboon (*Papio ursinus*) upper left incisor was thin sectioned and analyzed. The correspondence between LEH and AL defects is evaluated by comparing the association between these defect types on the enamel surface (LEH) and in the enamel cross-section (AL). Here we ask: (1) To what extent do LEH and AL defects co-occur on this baboon incisor? (2) Are rates of enamel extension, and associated striae angles, related to the distribution of LEH on the surface of this incisor? (3) Are this baboon's incisor striae angles acute and rates of enamel extension fast in comparison with those of great apes? Answers to these questions add to our understanding of the correspondence between AL and LEH defects, how much of a baboon's anterior tooth crown is likely to exhibit LEH in relation to AL, how fast baboon incisors grow, and how striae angles affect the manifestation of LEH defects.

Materials and Methods

The individual chosen for this analysis (identifier: B4-03) was a large (29.2 kg) male that lived in Table Mountain National Park near Cape Town and was euthanized for exhibiting aggressive behavior towards locals. This tooth was chosen for this histological study during the data collection phase of a larger study examining the difference in LEH prevalence between baboons living inside versus outside national parks. A second tooth (ULI1) from a different male chacma baboon (identifier: B2-03) was included in this study to measure midcrown striae of Retzius angles at the outer enamel surface.

An impression of the first upper left incisor (ULI1) (see Figure 2) was created using Coltene President Jet Light Body silicone impression material. The incisor's impression allowed for the creation of a high-resolution replica using Loctite EA E-60NC epoxy. Macrophotographs of the replica were acquired using a digital microscope (Leica DMS1000) and stitched using Adobe Photoshop CS6.

The replica was examined with the naked eye to identify LEH defects on the surface. Individual

LEH defects were assessed both with the naked eye and with the aid of macrophotographs. In this study, even minor perturbations involving the disruption of one or two perikymata growth increments were included in the LEH sample, which some authors might instead call "accentuated perikymata" (Thylstrup and Fejerskov, 1978; Kierdorf et al., 2000; Temple, 2014; O'Hara et al., 2023). A tripartite scheme was used to classify LEH defects as minor, moderate, or severe. The qualitative classification of LEH was made relative to other defects within the same tooth; comparing a given defect relative to other defects in the same tooth corrects for inter-tooth differences in growth and wear patterns. The position of an LEH defect along the length of the enamel was also considered, as seemingly shallow defects near the cusp of a heavily worn tooth are likely to be more severe (i.e., associated with a larger disruption in enamel formation) than their current state suggests.

The incisor was extracted by first securing the cranium to a laboratory bench and covering the tooth with padding material to prevent surface damage. The incisor was then pulled away from the cranium using locking flat pincers. After extraction, the incisor was embedded in Buehler EpoxiCure 2 epoxy. Using a Buehler Isomet low-speed saw, an initial cut was performed along the sagittal plane of the incisor at a speed of 90 revolutions per minute. One side of the halved tooth was then attached to a microscope slide using the same epoxy material.

The second cut was performed at the same angular speed and at a distance of 800 μm into the sectioned incisor relative to the surface of the microscope slide. The second cut yielded a thin section of the incisor 800 μm in thickness. After the sectioning process was complete, the specimen was attached to a target holder and ground to a thickness of 150 μm (thickness measurement includes thin section and epoxy adhesive) using progressively finer silicon carbide grinding paper. To minimize fine scratches, 0.3 μm alumina polishing compound was used to polish the slide in preparation for microscopy and imaging.

Using a brightfield microscope, images of the enamel were acquired at 4x magnification (1 pixel = 1.62 μm). FIJI (Preibisch et al., 2009) and Adobe Photoshop CS6 were used to stitch the images, producing a single image of the entire tooth section. The cuspal region is not preserved in this section due to normal wear (Figure 3). Therefore, the approximate location of the dentine horn was estimated by extending the trajectories of the labial and lingual enamel-dentine junctions until they

met. The reconstructed enamel-dentine junction length was measured and divided into deciles 1 through 10 (numbered from cusp to cervix) for analysis. Decile 1 and approximately half of the length of decile 2 constitute enamel lost to normal wear.

Enamel extension rates for the preserved deciles (3-10) were calculated by dividing the length of each decile (1/10 of the total length) by the number of days each decile took to form (Table 1). Days were calculated by counting the number of regular striae of Retzius in each decile and multiplying by the periodicity. Figure 4 shows the microscopic images of the enamel cross section obtained at 10x and 40x magnification to assess enamel periodicity, which was determined to be 7 days. This periodicity matches the previously reported value for the genus *Papio* (Dirks et al., 2002). The number of days it took for deciles 3-10 to form was also calculated by multiplying the number of striae in each decile by the periodicity (see Table 1). Striae angle measurements were taken within the middle of each decile directly below the outer enamel sur-

face. Using Adobe Photoshop, one arm of the angle tool was placed on the outer enamel surface while the other arm was extended along a single stria of Retzius approximately one third into the enamel thickness. Midcrown striae angles of another incisor (ULI1) from a different male chacma baboon (identifier: B2-03) were also measured at the outer enamel surface (the mean of the two specimens is reported in Table 3).

Accentuated lines (AL) appear as relatively dark and pronounced lines that do not follow the normal enamel formation rhythm (Guatelli-Steinberg, 2016). We attempted to score AL with the same level of sensitivity as we scored LEH defects; this meant that even minor AL were included in this sample. Lines were considered accentuated when they appeared out of the normal rhythm (i.e., there was an extra line between normal striae of Retzius) and/or when lines, whether falling with the normal rhythm or not, appear darker, thicker, and course more deeply into the enamel thickness compared to nearby striae of Retzius. Examples of AL defects are shown in Figure 5.

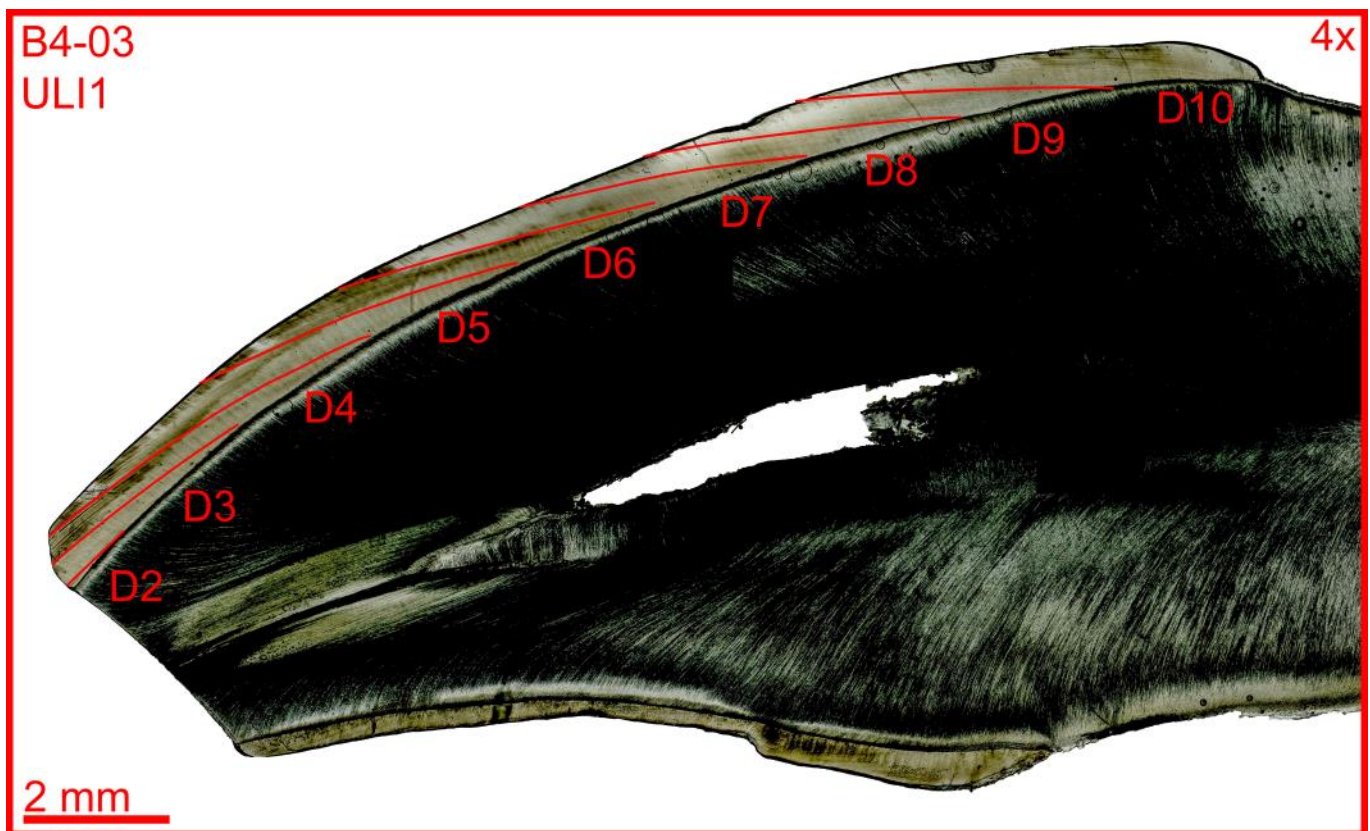


Figure 3. Overview montage of male chacma baboon B4-03 ULI1 thin section (4x magnification). Red lines mark the starting locations of deciles on the enamel-dentine junction and continue across the enamel to the points at which the striae of Retzius terminate on the outer enamel surface.

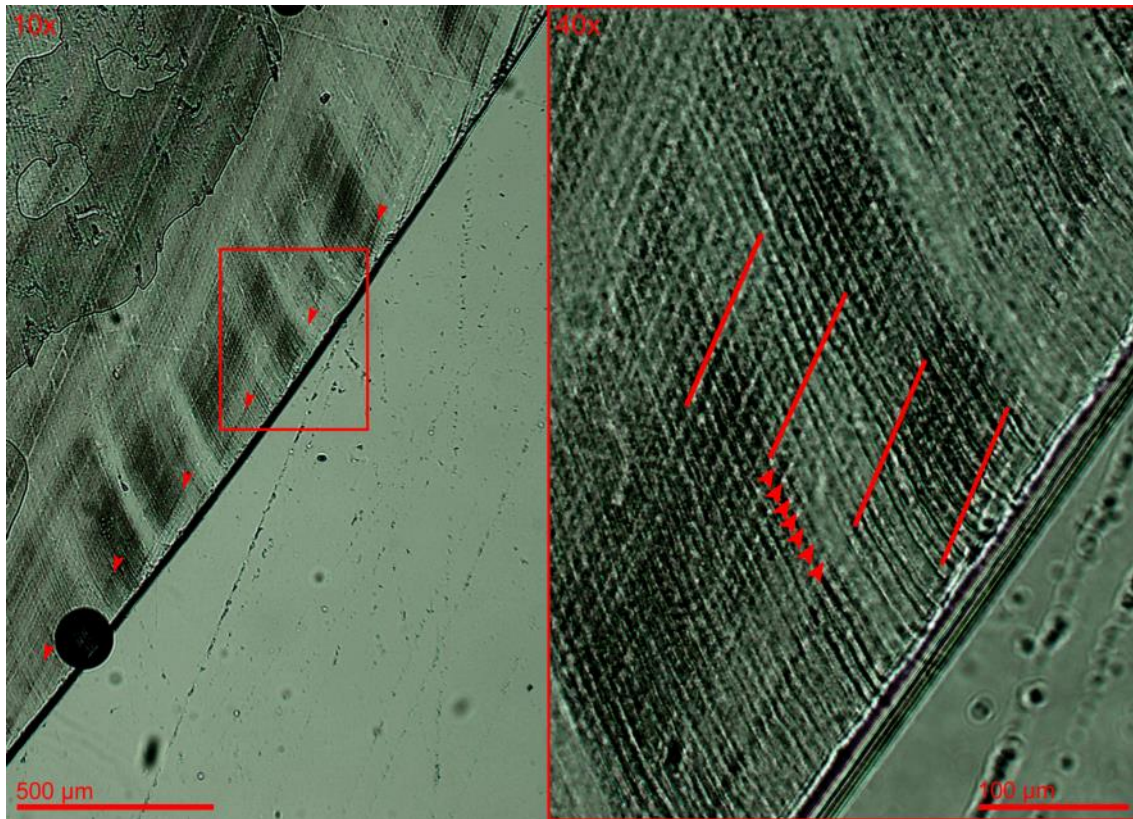


Figure 4. Left: 10x magnified image of B4-03 ULI1 with arrows showing the locations of striae of Retzius and rectangle denoting the region imaged at 40x magnification for periodicity assessment. Right: 40x magnified image with lines marking striae of Retzius and arrows marking daily cross striations. Daily cross striations were counted and measured to determine the periodicity of seven days.

Table 1. Mean striae of Retzius angles, enamel extension rates ($\mu\text{m}/\text{day}$), cumulative days of enamel formation, LEH defects, and AL defects per decile for B4-03 ULI1.

| Decile | Mean striae of Retzius angles | EER ($\mu\text{m}/\text{day}$) | Cumulative days (years) | LEH defects | AL defects |
|--------|-------------------------------|----------------------------------|-------------------------|-------------|------------|
| 3 | N/A | 43.9 | 49 (0.134) | 0 | 6 |
| 4 | N/A | 43.9 | 98 (0.268) | 0 | 5 |
| 5 | 10.7° | 17.1 | 224 (0.614) | 0 | 10 |
| 6 | 13.7° | 15.4 | 364 (0.997) | 1 | 7 |
| 7 | 14.0° | 16.2 | 497 (1.362) | 1 | 4 |
| 8 | 13.7° | 25.6 | 581 (1.592) | 2 | 5 |
| 9 | 15.3° | 18.1 | 700 (1.918) | 1 | 3 |
| 10 | 11.0° | 9.0 | 938 (2.570) | 5 | 8 |

In order to assess LEH and AL defect co-occurrence, the distance from the cementum-enamel junction to each LEH defect was recorded from the macrophotographs. The straight-line tool (Adobe Photoshop) was then dragged the same distance from the cementum-enamel junction visible in the thin section to the outer enamel surface where a surface groove was identified.

Results

There is a higher occurrence of accentuated lines (N = 48) compared to LEH defects (N = 10) in this chacma baboon first upper incisor. LEH defects were found to always co-occur with AL defects. Accentuated line defects are more evenly distributed throughout the enamel, while all LEH defects originated only within deciles 6-10 as defined at the enamel-dentine junction. However, due to the nature of crown development and curvature of striae, LEH defects are visible across much of the crown surface (see Figure 2). The frequency of LEH defects increases from cusp to cervix, with no defects originating in deciles 3-5, one defect per decile originating in deciles 6, 7, and 9, two defects origi-

nating in decile 8, and five defects originating in decile 10.

Table 1 (above) lists mean striae of Retzius angles for deciles 5 through 10. The most acute mean striae of Retzius angles are found in decile 5 (10.7°), while the most obtuse mean angles are found in decile 9 (15.3°). Table 1 also lists enamel extension rates (EER) and cumulative enamel formation days. Deciles 3 and 4 exhibited the highest EER in this tooth (43.9 $\mu\text{m}/\text{day}$), while decile 10 exhibited the lowest EER (9.0 $\mu\text{m}/\text{day}$). The mean EER across all deciles for B4-03 ULI1 is 23.6 $\mu\text{m}/\text{day}$, and is listed in Table 2 in comparison to mean EERs of anterior teeth of six other primate taxa derived from other studies. Midcrown striae of Retzius angles for the main subject of this study, individual B4-03, are 13.7°, while individual B2-03 had more acute midcrown angles at 13.3°. Mean midcrown striae angles are listed in Table 3 along with comparisons to the mean angles of anterior teeth of five other primate taxa derived from other studies.

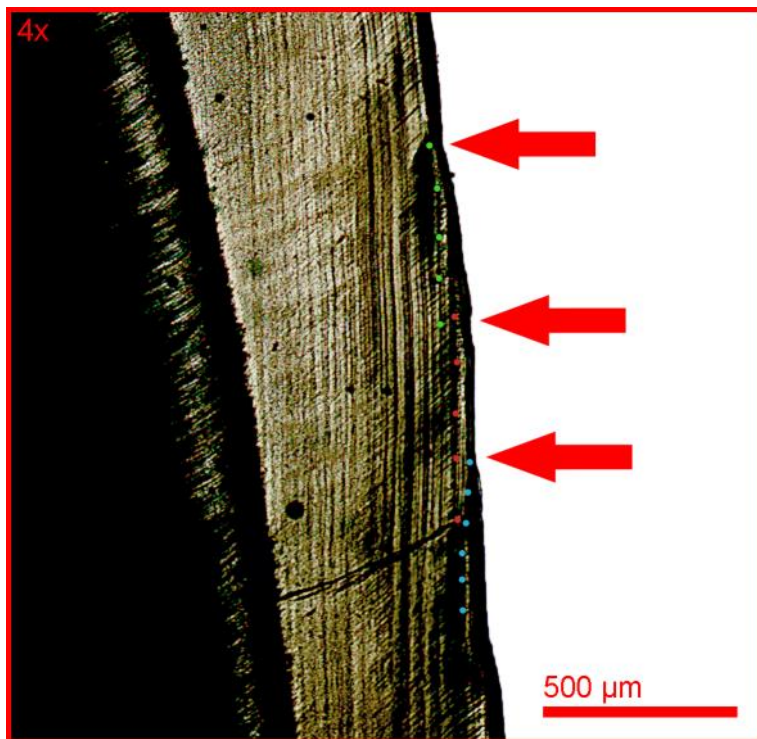


Figure 5. 4x magnified image of B4-03 ULI1. Red arrows mark the approximate locations of LEH defects on the outer enamel surface. Dotted red, green, and blue lines mark the approximate locations of AL defects in the enamel cross-section.

Table 2. Mean enamel extension rates (EER) in $\mu\text{m}/\text{day}$ for individual anterior teeth of six primate taxa.

| Taxon | Tooth type | Mean EER ($\mu\text{m}/\text{day}$) |
|---------------------------------------|------------|---------------------------------------|
| <i>Papio ursinus</i> | ULI1 | 23.6 |
| <i>Mandrillus sphinx</i> ¹ | LI1 | 15.5 |
| | LI2 | 14.9 |
| <i>G. b. beringei</i> ² | LC | 12.7 |
| <i>G. g. gorilla</i> ² | LC | 9.4 |
| <i>P. troglodytes</i> ² | LC | 8.6 |
| <i>Pongo sp.</i> ² | LC | 8.0 |

ULI1: upper left first incisor. LI1: lower first incisor. LI2: lower second incisor. LC: lower canine.

¹Dirks, Lemmers, Ngoubangoye, Herbert, and Setchell, 2020.

²McGrath et al., 2019

Table 3. Mean midcrown striae of Retzius angles in the anterior teeth of five primate taxa.

| Taxon | Tooth type | Number of specimens | Sex | Mean angle |
|-------------------------------------|-----------------|---------------------|------|------------|
| <i>Papio ursinus</i> | Central incisor | 2 | M | 13.5° |
| <i>G. b. beringei</i> ¹ | Canine | 2 | M | 18.5° |
| <i>Gorilla gorilla</i> ² | Central incisor | 4 | M, F | 18.0° |
| <i>Pan troglodytes</i> ² | Central incisor | 5 | M, F | 32.0° |
| <i>Pongo pygmaeus</i> ² | Central incisor | 4 | M, F | 45.0° |

¹McGrath et al. 2019.

²Guatelli-Steinberg et al., 2012.

Discussion

Specimen selection

This specific incisor (B4-03 ULI1) was chosen for this study for three reasons. First, the incisor contained a considerable number of LEH defects that are not confined to a small area of the outer enamel. This indicated that the enamel histology was likely to contain a number of AL defects that are also distributed throughout the enamel. These defects also varied in severity, allowing for the opportunity to find accentuated lines of varying severity. Second, incisors have relatively low EER compared to canines. Slow EERs (associated with relatively obtuse striae angles) may create LEH defects that are deeper and more defined (Guatelli-Steinberg et al., 2012; McGrath et al., 2019). In male primates, canines tend to have longer crown formation times compared to incisors (Ash and Nelson, 2003; Reed, 1973), allowing for the accrual of more LEH defects (Guatelli-Steinberg and Lukacs, 1998). However, this individual's canines contained a very large number of extremely shallow defects that often merged into indistinct grooves, preventing accurate discrimination of the boundaries of each defect. The third reason we chose an incisor (vs. a canine) for this study was a practical one; our low-speed saw was able to effectively cut the incisor, whereas the great length of the male chacma baboon canines prevented reliable sectioning using the available equipment.

Tooth wear: important considerations

In this study's main tooth of focus, normal tooth wear resulted in the loss of the first two enamel deciles and abrasion of the outer enamel surface, particularly near the cusp. This loss of enamel necessitates that the LEH and AL counts, as well as

the average enamel extension rate, are considered minimum values. Cuspal enamel usually has the fastest extension rate in primate teeth (Guatelli-Steinberg et al., 2012; McGrath et al., 2019; Shellis, 1998), meaning that the average EER reported in this study is likely lower than the actual rate due to the exclusion of the two lost cuspal deciles. The number of AL and LEH defects are also considered minimum counts in this study; since LEH, and particularly AL, defects are not confined to a limited section of the enamel, there are likely AL and LEH defects in the first two deciles that are not reported in this study.

EERs and LEH defect perceptibility

Large-bodied monkeys, such as baboons and mandrills, usually have higher average anterior teeth EERs than humans and extant great apes (Dirks et al., 2002; McGrath et al., 2019). Table 2 shows mean EERs for the anterior teeth of six primate taxa. The *Papio ursinus* upper incisor belonging to individual B4-03 exhibited the highest mean EER (23.6 $\mu\text{m}/\text{day}$) of all the primate taxa listed in Table 2, despite the fact that the first two deciles (i.e., those with the highest EER) had to be excluded due to wear. *Mandrillus sphinx*, the most closely-related species to *Papio ursinus* in Table 2, exhibits the second fastest mean EER (15.5 $\mu\text{m}/\text{day}$). Male *G. b. beringei* (mountain gorillas) canines have the highest EERs among the apes in Table 2 at 12.7 $\mu\text{m}/\text{day}$, but this is still lower than both of the aforementioned large-bodied monkey species. An examination of mountain gorilla incisors is needed in order to make direct comparisons with the data derived from the current study.

High EER is typically associated with relatively acute striae of Retzius angles, especially near the

cuspid. Table 3 shows the mean midcrown OES striae of Retzius angles in the anterior teeth of five primate taxa. The mean striae of Retzius angles of the two *Papio ursinus* central incisors measured in this study exhibit the most acute mean midcrown OES angles of all the taxa listed in Table 3 (13.3°). Male *G. b. beringei* canines exhibit the second most acute striae angles in Table 3 (18.5°), and are the acutest angles among the ape species listed. The very acute striae angles observed in these two incisors may produce very shallow LEH defects on the surface (Guatelli-Steinberg et al., 2012; McGrath et al., 2018, 2019), which are inherently less perceptible than deeper defects, particularly when using qualitative scoring methods. Since the main tooth in this study exhibits much faster EERs compared to apes, along with its acute striae angles, the difficulty in identifying LEH defects on the surface of this tooth can be attributed to, at least in part, the high EERs and acute striae angles found in this specimen.

The low perceptibility of shallow LEH in this tooth is further exacerbated by the intense feeding-induced teeth wear commonly seen in baboons. Since LEH defects are presumably very shallow in chacma baboons (though their depth is yet to be measured via profilometry), even relatively small amounts of tooth wear can obscure LEH defects. This is evident towards the cusp, as the cusp is naturally subject to more wear pressure compared to the cervical and middle sections of the incisor.

EERs and striae angles

The enamel extension rate gradient observed in this tooth likely contributed to more defined and deeper LEH defects in regions with low EER (midcrown and cervix) compared to regions with high EER (cusp). This is potentially another factor contributing to the difficulty in locating cuspal LEH defects. Interestingly, a disconnection is observed between striae of Retzius angles and EER, where, for example, the striae angles in deciles 7 and 8 are 14.0° and 13.7°, while the EERs are 16.2 and 25.6 $\mu\text{m}/\text{day}$, both respectively.

Striae of Retzius angles measured along the EDJ have been shown to serve as reliable proxies for EER estimations in human teeth (Boyde, 1964; Shellis, 1984), and at the OES, angles are strongly correlated with extension rates in ape canines (McGrath et al., 2019). However, individual-level variation in ameloblast cellular activity (i.e., variable rates of enamel matrix secretion) might influence EERs while not directly translating to a change in striae of Retzius angles. Other enamel

structure parameters also influence EER, such as the angle between the forming prisms and the EDJ or the length of enamel prism formed per day (Shellis, 1984), and may play a role in producing this unexpected decoupling between striae of Retzius angles and EER in this specimen. Future studies of multiple individuals will be able to assess whether this pattern occurs more broadly, and could incorporate measurements of daily secretion rates and geometric variables throughout the enamel thickness rather than just the OES.

Spatial distribution of AL and LEH defects

In this analysis, accentuated lines were evenly distributed throughout the enamel. Conversely, nine of the ten total LEH defects were observed in the middle and cervical sections of the outer enamel, while only one defect was observed in the cuspal third. This confinement of LEH distribution (which is not observed with accentuated line defects) can be attributed to a number of factors that serve to disconnect the two defect types, including the aforementioned dental wear. All but one of the LEH defects were classed as minor in severity, meaning that they represent short-lived growth disruptions only affecting a very small number of similar perikymata growth increments. This study did not attempt to classify AL based on their severity, though we did include even minor internal defects in the sample. Future studies could incorporate severity scoring into AL analyses to assess whether LEH occur in the absence of more marked AL, as has been proposed by Kierdorf et al. (2000, 2004) and Witzel et al. (2006, 2008), or if moderate to severe AL usually underlie LEH, as demonstrated by Smith and Boesch (2015).

In permanent upper central incisors, enamel at the cusp is composed mostly of appositional enamel, while the remainder of the crown is composed mainly of imbricational enamel (Hillson and Bond, 1997). During the formation of appositional enamel, stress-associated enamel formation impairment may never manifest as LEH on the surface, as the striae of Retzius do not terminate at the outer enamel surface as is the case with imbricational enamel (Witzel et al., 2008). This key difference suggests that histological examination of accentuated lines (as opposed to surface examination of LEH) in teeth regions composed of appositional enamel is necessary to identify stress markers that do not extend to the OES. In this study, the cuspal enamel could not be analyzed due to wear, so the remaining eight deciles are comprised of entirely imbricational enamel where LEH defects could

manifest on the surface.

Future directions

Future work will focus on expanding the sample size to include more individuals and several other tooth types. Incorporating life records of tracked individual baboons in both anthropogenic and rural environments can help in drawing connections between documented stress episodes (e.g., malnutrition, illness, or physical injury) and specific LEH or AL defects.

It is important to note that accentuated lines and LEH defects are disruptions in the normal enamel growth rate, meaning they can only manifest as the enamel is actively growing. Consequently, the physiological stress episodes that resulted in LEH and AL defects happened within the developmental window of the examined tooth. Different tooth types have different, and sometimes non-overlapping, windows of development (Reed, 1973). Examination of a set of teeth from one individual can help with identifying stress episodes occurring over a larger span of an animal's life compared to the examination of only a single tooth.

Profilometric analysis of the enamel surface can aid in the process of identifying LEH defects in general (e.g., McGrath et al., 2018), and especially toward the cusp where they tend to be either very shallow due to cuspal enamel geometry or obscured by normal tooth wear. Profilometry can also be helpful in providing quantitative measurements of the various topographical characteristics of the enamel (defect depth, width, regularity, etc.), allowing for better definition of criteria for minor, moderate, and severe defects.

Conclusions

We found a higher occurrence of internal AL (N = 48) compared to external LEH defects (N = 10), which co-occurred in all instances of LEH. Despite the loss of the first two deciles to normal wear, this incisor exhibited a fast mean EER of 23.6 $\mu\text{m}/\text{day}$, which is faster than several large-bodied monkey species reported in other studies (see Table 2). With the inclusion of a second specimen for mid-crown OES striae angle measurements, the mean angle measured was more acute than several primate taxa reported in other studies (see Table 3). LEH and AL counts and mean EER reported in this study are considered minimum values, as enamel loss and surface abrasion prevented the analysis of the first two deciles, which likely exhibited the fastest EERs and contained additional enamel de-

fects. We offer the findings of this study as an initial exploration of the questions set out in the introduction, as our sample size is small. Future work will expand sample size, utilize profilometric analysis of the enamel surface, and incorporate detailed life records of individual baboons to investigate links between documented stress episodes and LEH or AL defects.

Funding sources

This project received funding from the Ohio State University President's Postdoctoral Scholars Program and NSF Grant 1945008.

References

- Ash, M., & Nelson, S. (2003). *Wheeler's Dental Anatomy, Physiology, and Occlusion* (8th ed., p. 32). St. Louis, Missouri: Saunders.
- Beamish, E., & O'Riain, M. (2014). The Effects of Permanent Injury on the Behavior and Diet of Commensal Chacma Baboons (*Papio ursinus*) in the Cape Peninsula, South Africa. *International Journal of Primatology*, 35(5), 1004-1020. doi: 10.1007/s10764-014-9779-z
- Boyde, A. (1964). *The Structure and Development of Mammalian Enamel*. PhD Thesis, University of London, London, England.
- Chowdhury, S., Brown, J., & Swedell, L. (2020). Anthropogenic effects on the physiology and behaviour of chacma baboons in the Cape Peninsula of South Africa. *Conservation Physiology*, Volume 8, Issue 1, 2020, coaa066. doi:10.1093/conphys/coaa066
- Condon, K., & Rose, J. C. (1992). Intertooth and intratooth variability in the occurrence of developmental enamel defects. *Journal of Paleopathology*, 2, 61-77.
- Daegling, D., & Grine, F. (1999). Terrestrial foraging and dental microwear in *Papio ursinus*. *Primates*, 40(4), 559-572. doi: 10.1007/bf02574831
- Dirks, W., Lemmers, S., Ngoubangoye, B., Herbert, A., & Setchell, J. (2020). Odontochronologies in male and female mandrills (*Mandrillus sphinx*) and the development of dental sexual dimorphism. *American Journal of Physical Anthropology*, 172(4), 528-544. doi: 10.1002/ajpa.24094
- Dirks, W., Reid, D. J., Jolly, C. J., Phillips-Conroy, J. E., & Brett, F. L. (2002). Out of the mouths of baboons: stress, life history, and dental development in the Awash National Park hybrid zone, Ethiopia. *American Journal of Physical Anthropology*, 118(3), 239-252. doi: 10.1002/

- ajpa.10089
- Dumont, E. R. (1995). Mammalian enamel prism patterns and enamel deposition rates. *Scanning Microscopy*: Vol. 9: No. 2, Article 12. Retrieved from <https://digitalcommons.usu.edu/microscopy/vol9/iss2/12>
- Galbany, J., Romero, A., Mayo-Alesón, M., Itsoma, F., Gamarra, B., Pérez-Pérez, A., Willaume, E., Kappeler, P. M., & Charpentier, M. J. (2014). Age-Related Tooth Wear Differs between Forest and Savanna Primates. *PLoS ONE*, 9(4), e94938. doi: 10.1371/journal.pone.0094938
- Goodman A.H., & Rose J.C. (1990). Assessment of systemic physiological perturbations from dental enamel hypoplasias and associated histological structures. *Yearbook of Physical Anthropology*, 33: 59-110. doi: 10.1002/ajpa.1330330506
- Guatelli-Steinberg, D. (2016). Chapter 27: Dental Stress Indicators from Micro- to Macroscopic. In J. D. Irish & G. R. Scott (Eds.), *A Companion to Dental Anthropology* (pp. 450–457). West Sussex, UK: Wiley Blackwell.
- Guatelli-Steinberg, D., & Lukacs, J. R. (1998). Preferential expression of linear enamel hypoplasia on the sectorial premolars of rhesus monkeys (*Macaca mulatta*). *American Journal of Physical Anthropology*, 107(2), 179–186. doi: 10.1002/(sici)1096-8644(199810)107:2<179::aid-ajpa4>3.0.co;2-q
- Guatelli-Steinberg, D., Ferrell, R., & Spence, J. (2012). Linear enamel hypoplasia as an indicator of physiological stress in great apes: reviewing the evidence in light of enamel growth variation. *American Journal of Physical Anthropology*, 148(2), 191-204. doi: 10.1002/ajpa.21619
- Hillson, S., & Bond, S. (1997). Relationship of enamel hypoplasia to the pattern of tooth crown growth: A discussion. *American Journal of Physical Anthropology*, 104(1), 89-103. doi: 10.1002/(sici)1096-8644(199709)104:1<89::aid-ajpa6>3.0.co;2-8
- Hoffman, T. S., & O’Riain, M. J. (2011). The spatial ecology of chacma baboons (*Papio ursinus*) in a human-modified environment. *International Journal of Primatology*, 32(2), 308-328. doi: 10.1007/s10764-010-9467-6
- Hoffman, T. S., & O’Riain, M. J. (2012). Troop size and human-modified habitat affect the ranging patterns of a chacma baboon population in the cape peninsula, South Africa. *American Journal of Primatology*, 74(9), 853–863. doi: 10.1002/ajp.22040
- Kansky, R., & Gaynor, D. (2000). *Baboon management strategy for the Cape Peninsula* (Final Report, Table Mountain Fund Project No. ZA 568). Table Mountain Fund, Cape Town, South Africa.
- Kierdorf, H., Kierdorf, U., Richards, A., & Josephsen, K. (2004). Fluoride-induced alterations of enamel structure: an experimental study in the miniature pig. *Anatomy And Embryology*, 207(6), 463-474. doi: 10.1007/s00429-003-0368-8
- Kierdorf, H., Kierdorf, U., Richards, A., & Sedlacek, F. (2000). Disturbed enamel formation in wild boars (*Sus scrofa* L.) from fluoride polluted areas in central Europe. *The Anatomical Record*, 259(1), 12-24. doi: 10.1002/(sici)1097-0185(20000501)259:1<12::aid-ar2>3.0.co;2-6
- Lucas, P., Constantino, P., Wood, B., & Lawn, B. (2008). Dental enamel as a dietary indicator in mammals. *BioEssays*, 30(4), 374-385. doi: 10.1002/bies.20729
- Mahoney, P., Miszkiewicz, J. J., Pitfield, R., Deter, C., & Guatelli-Steinberg, D. (2017). Enamel biorhythms of humans and great apes: the Havers-Halberg Oscillation hypothesis reconsidered. *Journal of Anatomy*, 230(2), 272–281. doi: 10.1111/joa.12551
- McGrath, K., El-Zaatari, S., Guatelli-Steinberg, D., Stanton, M. A., Reid, D. J., Stoinski, T. S., Cranfield, M. R., Mudakikwa, A., & McFarlin, S. C. (2018). Quantifying linear enamel hypoplasia in Virunga Mountain gorillas and other great apes. *American Journal of Physical Anthropology*, 166(2), 337–352. doi: 10.1002/ajpa.23436
- McGrath, K., Reid, D., Guatelli-Steinberg, D., Arbenz-Smith, K., El Zaatari, S., & Fatica, L. et al. (2019). Faster growth corresponds with shallower linear hypoplastic defects in great ape canines. *Journal of Human Evolution*, 137, 102691. doi: 10.1016/j.jhevol.2019.102691
- Molnar, P. (2011). Extramasticatory dental wear reflecting habitual behavior and health in past populations. *Clinical Oral Investigations*, 15(5), 681–689. doi: 10.1007/s00784-010-0447-1
- Nanci, A. (2018). *Ten Cate’s Oral Histology: Development, Structure, and Function* (9th ed., pp. 152-154). St. Louis, Missouri: Elsevier.
- O’Hara, M. C., McGraw, W. S., & Guatelli-Steinberg, D. (2023). Some orangutans acquire enamel defects at regular intervals, but not according to seasonal cycles. *American Journal of Biological Anthropology*, 1–15. doi: 10.1002/ajpa.24690
- Preibisch, S., Saalfeld, S., & Tomancak, P. (2009). Globally optimal stitching of tiled 3D microscopic image acquisitions. *Bioinformatics*, 25

- (11), 1463-1465. doi: 10.1093/bioinformatics/btp184
- Reed, O. M. (1973). *Papio cynocephalus* age determination. *American Journal of Physical Anthropology*, 38(2), 309-314. doi: 10.1002/ajpa.1330380226
- Risnes, S. (1990). Structural characteristics of staircase-type Retzius lines in human dental enamel analyzed by scanning electron microscopy. *The Anatomical Record*, 226(2), 135-146. doi: 10.1002/ar.1092260203
- Shellis, R. P. (1984). Variations in growth of the enamel crown in human teeth and a possible relationship between growth and enamel structure. *Archives of Oral Biology*, 29(9), 697-705. doi: 10.1016/0003-9969(84)90175-4
- Shellis, R. P. (1998). Utilization of periodic markings in enamel to obtain information on tooth growth. *Journal of Human Evolution*, 35(4-5), 387-400. doi: 10.1006/jhev.1998.0260
- Skead, C. J. (1980). *Historical mammal incidence in the Cape Province* (Vol. 1). Cape Town, South Africa: Department of Nature and Environmental Conservation of the Provincial Administration of the Cape of Good Hope.
- Smith, T.M. & Boesch, C. (2015). Developmental defects in the teeth of three wild chimpanzees from the Taï forest. *American Journal of Physical Anthropology*, 157: 556-570. doi: 10.1002/ajpa.22741
- Stojanowski, C. M., Johnson, K. M., Paul, K. S., & Carver, C. L. (2016). Chapter 23: Indicators of Idiosyncratic Behavior in the Dentition. In J. D. Irish & G. R. Scott (Eds.), *A Companion to Dental Anthropology* (pp. 381-382). West Sussex, UK: Wiley Blackwell.
- Strum, S. C. (2010). The Development of Primate Raiding: Implications for Management and Conservation. *International Journal of Primatology*, 31(1), 133-156. doi: 10.1007/s10764-009-9387-5
- Temple, D.H. (2014). Plasticity and constraint in response to early-life stressors among late/final Jomon period foragers from Japan: Evidence for life history trade-offs from incremental microstructures of enamel. *American Journal of Physical Anthropology*, 155: 537-545. doi: 10.1002/ajpa.22606
- Thylstrup, A. & Fejerskov, O. (1978). Clinical appearance of dental fluorosis in permanent teeth in relation to histologic changes. *Community Dentistry and Oral Epidemiology*, 6: 315-328. doi: 10.1111/j.1600-0528.1978.tb01173.x
- Ungar, P. (1994). Patterns of ingestive behavior and anterior tooth use differences in sympatric anthropoid primates. *American Journal of Physical Anthropology*, 95(2), 197-219. doi: 10.1002/ajpa.1330950207
- Witzel, C., Kierdorf, U., Dobney, K., Ervynck, A., Vanpoucke, S., & Kierdorf, H. (2006). Reconstructing impairment of secretory ameloblast function in porcine teeth by analysis of morphological alterations in dental enamel. *Journal of Anatomy*, 209(1), 93-110. doi: 10.1111/j.1469-7580.2006.00581.x
- Witzel, C., Kierdorf, U., Schultz, M., & Kierdorf, H. (2008). Insights from the inside: Histological analysis of abnormal enamel microstructure associated with hypoplastic enamel defects in human teeth. *American Journal of Physical Anthropology*, 136(4), 400-414. doi: 10.1002/ajpa.20822